BMC Genomics

RESEARCH

Open Access

Chromosome-level genome provides new insights into the fatty acid biosynthesis and metabolism of the sea urchin *Strongylocentrotus intermedius*

Lingshu Han[1,2,3†], Jun Ding[1,2,3*†], Heng Wang[1,2,3†], Yang Zhang[1,2,3], Junxiao Sun[1,2,3], Chong Zhao[1,2,3], Weijie Zhang[1,2,3], Rantao Zuo[1,2,3], Wenpei Wang[1,2,3], Ye Tian[1,2,3] and Yaqing Chang[1*]

Abstract

Polyunsaturated fatty acids (PUFAs) are important nutrients that play critical roles in sea urchin reproduction and early development. *Strongylocentrotus intermedius*, the only commercially cultured sea urchin species in China with substantial economic value, has edible gonads that are particularly rich in PUFAs.

In this study, we investigated the molecular mechanisms underlying fatty acid biosynthesis and metabolism through chromosome-level genome assembly, evolutionary analysis, and transcriptomic profiling across developmental and gonadal stages. We assembled a chromosome-level genome (704.9 Mb; Scaffold N50 30 Mb) and identified an expansion of the *Elovl* gene family, indicating a strong endogenous capacity for fatty acid synthesis. To systematically characterize metabolic changes during gonadal development, raw RNA-seq data from previously published gonadal samples were re-analyzed together with newly generated stage 4 gonadal samples. Pathway analysis revealed that unsaturated fatty acid biosynthesis was more active during early gonadal development in males, whereas in females it remained elevated during later developmental stages, suggesting that females maintain sustained fatty acid biosynthesis throughout gonadal development, while males prioritize rapid sperm production at immature stages. During larval development, the expression of key fatty acid synthesis genes (*Fads*, *Elovl5*, *Elovl4*, and *ACSL6*) gradually decreased as planktonic larvae transitioned to benthic juveniles and endogenous lipid reserves were progressively consumed, reflecting metabolic adaptation to environmental and developmental changes.

Collectively, these findings advance our understanding of fatty acid metabolism in echinoderms and provide a valuable genomic and transcriptomic resource for future studies on lipid biosynthesis and metabolism in marine invertebrates.

†Lingshu Han, Jun Ding and Heng Wang contributed equally to this work.

*Correspondence:
Jun Ding
dingjun19731119@hotmail.com
Yaqing Chang
yqchang@dlou.edu.cn

Full list of author information is available at the end of the article

Keywords *Strongylocentrotus intermedius*, Chromosome-level genome assembly, Development, Fatty acid synthesis and metabolism

Introduction

The sea urchin *Strongylocentrotus intermedius*, characterized by rapid growth and high gonad quality, is currently the only sea urchin species commercially cultured in China and therefore holds substantial economic value. In sea urchin aquaculture, larval survival and gonadal nutrient accumulation are key determinants of production yield and product quality [1], underscoring the importance of understanding the molecular mechanisms underlying fatty acid biosynthesis and metabolism.

Polyunsaturated fatty acids (PUFAs) play essential roles in sea urchin gonadal development, serving both as structural components of cellular membranes and as major energy reserves. As the primary lipid storage organ, the gonads accumulate large quantities of PUFAs to support gametogenesis [2]. In *S. intermedius*, levels of free fatty acids and triglycerides—major transport and storage forms of PUFAs—decline markedly after spawning, whereas cholesterol, a key molecule involved in steroid hormone production and membrane synthesis, increases significantly in female gonads [3]. Integrated metabolomic and transcriptomic analyses have further demonstrated that genes involved in PUFA biosynthesis and metabolism exhibit dynamic and stage-specific expression patterns during gonadal development, revealing a tightly regulated energy allocation network that supports gamete maturation [4, 5].

In addition to their role in reproduction, gonadal PUFAs are crucial for early embryonic development in sea urchins. Fatty acids serve as primary metabolic substrates for oocytes and early embryos, where maternally derived lipids are mobilized through enzymatic hydrolysis to provide both energy and membrane components. In the green sea urchin *Evechinus chloroticus*, substantial triglyceride consumption occurs during the transition from early to late 4-arm larval stages, coinciding with the formation of fully developed arms and intestines. During the 8-arm larval stage, neutral lipids and free fatty acids accumulated to meet the energetic demands of metamorphosis [6]. Similarly, in *Tripneustes gratilla*, lipid and protein consumption is minimal during early embryogenesis; however, approximately 50% of maternal lipid reserves are depleted by the two-arm larval stage, and nearly all maternal nutrients are exhausted by the 4-arm stage [7].

Although previous studies have demonstrated that *S. intermedius* possesses endogenous PUFA biosynthetic capacity and that lipid metabolic pathways were largely conserved among sea urchins [8, 9], the precise molecular networks and regulatory dynamics governing fatty acid synthesis and metabolism remain poorly understood. Addressing these knowledge gaps requires high-quality genomic and transcriptomic resources. In this study, we constructed a chromosome-level genome assembly of *S. intermedius* and generated comprehensive transcriptomic profiles spanning gonadal and larval developmental stages to investigate the regulatory mechanisms underlying fatty acid synthesis and metabolism during reproduction and early development. This work expands genomic resources for echinoderms, clarifies endogenous fatty acid biosynthetic pathways in sea urchins, and provides a theoretical foundation for the selective breeding of sea urchin varieties enriched in polyunsaturated fatty acids.

Materials and methods

Sample collection

Collection of samples for genome sequencing and annotation

Healthy 2-year-old *S. intermedius* (average test diameter: 56.72 ± 1.65 mm, average test height: 32.35 ± 1.58 mm, weight: 55.08 ± 2.88 g) (Fig. 1A) were acquired in 2019 from Dalian Haibao Fishery Co., Ltd. (38°91'25"N, 121°60'25"E) in Dalian, Liaoning Province, China, and were immediately transported to the Key Laboratory of Mariculture & Stock Enhancement in the North China Sea, Ministry of Agriculture and Rural Affairs, Dalian Ocean University, Dalian, Liaoning, China.

To obtain sperm for genome sequencing, three *S. intermedius* were injected with 1 mL of KCl (40 μL/g body weight) through the perioral membrane into the body cavity to induce spawning. Sperm was collected using a pipette into a 2 mL centrifuge tubes and liquefied at 37 °C water bath for 30 min, centrifuged at 1500 × g for 20 min. The supernatant was removed, the sperm pellet was retained, rapidly frozen in liquid nitrogen, and store at -80 °C for subsequent experiments.

For auxiliary genome annotation, three *S. intermedius* were dissected, and five different tissues (tube foot, peristomial membrane, gonad, digestive tract, and Aristotle's lantern) were collected into 2 mL centrifuge tubes. These were rapidly frozen in liquid nitrogen and stored at -80 °C in an ultra-low temperature freezer for subsequent auxiliary annotation.

Collection of gonadal samples at the mature developmental stage

Healthy 2-year-old *S. intermedius* were purchased in August 2022 from Dalian Haibao Co., Ltd. (Dalian, China). After transportation to the laboratory, sea urchins were maintained in 1000-L tanks at 15 ± 0.5 °C

Table 1 Summary of sequencing data for *S. intermedius* genome assembly

Paired-end libraries	Insert size (bp)	Total data (Gb)	Read length (bp)	Sequence coverage (×)
Illumina reads	350	121.37	150	186.07
PacBio reads	20,000	115.94	16,920	164.47
Hi-C	300–700	111.68	150	158.44
Total		348.99		508.98

and 31 ± 0.5‰ salinity, and were fed continuously with kelp (*Laminaria japonica*) throughout the experiment. Gonadal sex and developmental stage were determined according to previously described criteria [4]. Only gonads at the mature stage (stage 4) were used in this study. At this stage, the gonadal lumen is filled with fully differentiated and stored mature ova or immotile spermatozoa.

Gonadal tissues were collected in October 2022. Portions of gonadal tissue were rapidly frozen in liquid nitrogen and stored at -80 °C for subsequent RNA extraction. In parallel, portions of gonadal tissue were fixed in Bouin's solution, embedded in paraffin, sectioned at 6 μm, and stained with hematoxylin and eosin (HE; Institute of Biological Sciences, Suzhou, Jiangsu). Sex and gonadal developmental stage were confirmed under a microscope based on histological observations. Based on the observation results, the mature-stage female and male samples used in this study were named Ost4 and Tst4, respectively (Fig. 5A). Three female and three male samples at stage 4 of gonadal development were selected for transcriptomic sequencing analysis.

Collection of samples from different developmental stages

To collect samples from various developmental stages, three females and three males were induced to spawn through an injection of 1 mL KCl (0.5 mol/L, 40 μL/g of body mass [10]) into the coelom via the peristomial membrane [11] in March 2020. Sea urchin larvae samples at 15 different developmental stages, including fertilized egg (FE), 2 cell stage (CS-2), 4 cell stage (CS-4), 8 cell stage (CS-8), 16 cell stage (CS-16), 32 cell stage (CS-32), multicellular stage (MS), blastula stage (BS), gastrula stage (GS), prism larvae (PL), 2-armed larvae (AL-2), 4-armed larvae (AL-4), 6-armed larvae (AL-6), 8-armed larvae (AL-8), juvenile sea urchin (JSU), were collected for transcriptome analysis (Fig. 6A) [12]. Samples were pooled, passed through a 400 μm sieve to remove impurities, collected with pipettes, and placed in 1.5 mL centrifuge tubes. All tissue and stage samples were immediately frozen in liquid nitrogen and stored at -80 °C prior to RNA extraction and fatty acid analyses.

Genome sequencing and analysis

Genomic DNA was extracted from *S. intermedius* sperm using the cetyl trimethyl ammonium bromide (CTAB) method. The CTAB method is a widely used technique for DNA extraction, primarily involving the dissolution of cell membranes using CTAB and the selective precipitation of DNA under varying salt conditions [13]. DNA quality and integrity were assessed using agarose gel electrophoresis and a Qubit fluorometer.

Illumina short-read sequencing

Short-insert paired-end libraries with an average insert size of approximately 350 bp were constructed according to the manufacturer's instructions and sequenced on the NovaSeq 6000 platform (Illumina, CA, USA) with a read length of 2 × 150 bp. Raw reads were subjected to quality control to remove adapter sequences, low-quality reads, and reads containing excessive ambiguous bases, generating high-quality clean reads for downstream analyses.

PacBio long-read sequencing

For long-read sequencing, high-molecular-weight genomic DNA (10 μg) was used for PacBio library construction. DNA damage repair, end repair, and adapter ligation were performed using the PacBio Express Template Prep Kit 2.0. Size selection of 15–20 kb fragments was conducted using the BluePippin Size-Selection System (Sage Science). The size-selected libraries were purified with AMPure PB beads and assessed for concentration and fragment size distribution. Sequencing-ready libraries were bound with primers and polymerase using the PacBio Sequel II Binding Kit 2.0 and sequenced on the PacBio Sequel II platform in continuous long-read (CLR) mode. A total of 115.94 Gb of high-quality PacBio CLR data were generated, corresponding to approximately 164.47× genome coverage.

Genome assembly and polishing

PacBio CLR reads were first corrected using Canu (version 1.5) [14]. De novo genome assembly was then performed using wtdbg2 (https://github.com/ruanjue/wtdbg2), which constructs a fuzzy de Bruijn graph optimized for long noisy reads. The initial assembly was further refined through sequence alignment using MUMmer (version 4.0.0) [15]. To further improve assembly accuracy, Illumina short reads were aligned to the assembled genome using BWA (https://bio-bwa.sourceforge.net/bwa.shtml) [16] and sequence polishing was performed to correct potential base-level errors. The resulting polished assembly was used for subsequent scaffolding and analyses.

Hi-C library construction and chromosome-level scaffolding

To generate chromosome-level assemblies, Hi-C libraries with insert sizes ranging from 300 to 700 bp were constructed from *S. intermedius* sperm following the protocol [6]. Hi-C libraries were sequenced on the NovaSeq6000 (Illumina, CA, USA) platform using paired-end reads. Raw Hi-C reads were filtered to remove adapter contamination and low-quality reads. Clean reads were aligned to the polished genome assembly, and invalid read pairs, including dangling-end, self-cycle, re-ligation, and dumped products, were filtered using HiC-Pro (version 2.8.1) [17]. The remaining valid interaction pairs were used for chromosome-level scaffolding. Scaffolds were clustered, ordered, and oriented into chromosome-scale assemblies using Lachesis (version 1.0) [18]. Default parameters were applied unless otherwise specified.

Genome assembly evaluation

To evaluate the quality of the chromosome-level genome assembly, Illumina short reads were mapped back to the final assembly using BWA (version 0.7.10-r789). Mapping statistics were calculated to assess assembly accuracy and completeness. Genome completeness was further assessed using BUSCO (version 2.0) [19] with the *metazoa*_odb10 dataset, which contains 954 conserved single-copy orthologs. The proportion of complete, fragmented, and missing BUSCO genes was used as an indicator of assembly quality.

Repeat annotation, gene prediction and functional annotation

Repeat annotation

Repetitive elements in the *S. intermedius* genome were identified using a combination of de novo and homology-based approaches. A species-specific repeat library was constructed using LTR_FINDER (version 1.05) and RepeatScout (version 1.0.5) [20]. Repeat sequences were classified using PASTEClassifier (version 2.0) integrated with the Repbase database (version 19.06) [21]. The final repeat library was used to identify and mask repetitive elements in the genome using RepeatMasker (version 4.2.1) [22].

Gene prediction, and functional annotation

Protein-coding genes were predicted through a combined approach: (1) *de novo* prediction using Genscan (version 3.1.2) [23], Augustus (version 2.4) [24], GlimmerHMM (version 3.0.4), GeneID (version 1.4) and SNAP (version 2006-07-28) [25]; (2) homology-based prediction with GeMoMa (version 1.9) [26] against proteins from *Apostichopus japonicus* (GCA_002754855.1), *Strongylocentrotus purpuratus* (GCA_000002235.4), and *Acanthaster planci* (GCA_001949145.1); (3) transcriptome-based gene prediction was carried out using RNA-seq data from five *S. intermedius* tissues. TransDecoder (version 2.0), GeneMarkS-T (version 5.1) [27], and PASA (version 2.0.2) [28] were employed to predict gene models based on transcript evidence. Predictions were integrated by EvidenceModeler (EVM) and refined with PASA (version 2.5.3) [29]. Non-coding RNAs included miRNA/rRNA identified by Rfam alignment, tRNA detected with tRNAscan-SE (version 2.0) [30], and pseudogenes screened by GenBlastA (version 1.39) [31] followed by premature stop codon/frameshift validation via GeneWise (version 2.4.0) [32]. Functional annotation of predicted protein-coding genes was performed by sequence similarity searches against the NCBI non-redundant protein (NR), KOG, and other public databases using BLAST. Functional assignments were based on the best hits obtained from these databases.

Comparative genomics analysis

We conducted a comparative genomics analysis using the protein sequences of 11 species from NCBI (https://www.ncbi.nlm.nih.gov/bioproject/): *S. intermedius* (PRJNA1356650), *Lytechinus pictus* (PRJNA1092071), *Lytechinus variegatus* (PRJNA1111502), *Anneissia japonica* (PRJNA615663), *A. japonicus* (PRJNA1390431), *S. purpuratus* (PRJNA1308562), *A. planci* (PRJNA1039947), *Patiria miniate* (PRJNA1244632), *Branchiostoma lanceolatum* (PRJNA1134169), *Danio rerio* (PRJNA1423909), and *Crassostrea gigas* (PRJNA1354972). The selected species cover five classes of echinoderms, chordates, and mollusks, tracing evolutionary nodes from basal deuterostomes (sea urchins) to vertebrates (zebrafish). Gene family clustering was performed using OrthoFinder (version 2.4) [33]. Single-copy orthologous genes from all 11 species were aligned using MAFFT (version 7.205) [34]. The protein sequence alignments were then converted into codon alignments using PAL2NAL (version 14) [35]. We applied Gblocks (version 0.91b) [36] to remove low-quality sequences and highly divergent regions to ensure the accuracy of the alignment.

A maximum likelihood phylogenetic tree was constructed using IQ-TREE (version 1.6.11) [37] with the LG + F+I+G4 model. Fossil records and divergence times were retrieved from the TimeTree database (http://www.timetree.org/) to estimate divergence times between *S. intermedius* and other species, which was further refined using the MCMCtree tool in PAML (version 4.9i) [38]. Based on the constructed phylogenetic tree, we identified expanded and contracted gene families using CAFE (version 4.2). To analyze positive selection, we employed the codeml program in PAML, utilizing the F3 × 4 model of codon frequencies.

Transcriptome sequencing and analysis

Total RNA was extracted, quality assessed, and purified following the Ye's method [39]. Total RNA was extracted from gonadal samples at different developmental stages and from embryonic/larval samples using TRIzol reagent (Invitrogen, USA) following a standardized protocol. For gonadal tissues, approximately 100 mg of tissue was homogenized in liquid nitrogen prior to extraction. For embryonic and larval samples, individuals were collected at each defined developmental stage, rinsed three times with sterile phosphate-buffered saline (PBS) to remove debris, rapidly frozen in liquid nitrogen, and homogenized thoroughly before RNA extraction. Homogenized samples were mixed with 1 mL TRIzol reagent and incubated for 5 min at room temperature. Chloroform (0.2 mL) was added for phase separation, followed by centrifugation at 12,000 × g for 10 min at 4 °C. The aqueous phase was transferred to a new tube, and RNA was precipitated with an equal volume of isopropanol. The RNA pellet was washed with 75% ethanol, air-dried, and dissolved in RNase-free water. Residual genomic DNA was removed by DNase I treatment. RNA quality and integrity were assessed prior to library construction.

RNA sequencing datasets

Two transcriptome datasets were analyzed in this study: (1) Gonadal developmental-stage transcriptome dataset: This dataset included gonadal samples from developmental stages Ost1–Ost3 and Tst1–Tst3 generated in our previous study [4] using paired-end sequencing on the Illumina HiSeq 4000 platform, as well as newly generated mature-stage samples (Ost4 and Tst4) sequenced on the NovaSeq 6000 platform (Illumina, CA, USA). To ensure consistency, raw FASTQ files from the published samples and newly generated samples were combined and re-analyzed using the same bioinformatics pipeline. (2) Larval developmental transcriptome dataset: Larval samples were sequenced using paired-end sequencing on the Illumina NovaSeq 6000 platform (Illumina, CA, USA).

Quality control and read alignment

Raw sequencing reads from all datasets were first processed using fastp to remove adapter sequences, reads with more than 10% ambiguous bases, and reads with low-quality scores ($Q < 20$). Only high-quality clean reads were retained for downstream analyses.

Clean reads were aligned to the assembled reference genome using TopHat2 (version 2.1.1) with default parameters to enable splice-aware alignment [40]. TopHat2 remains suitable for reference-based transcriptome analysis and provides reliable mapping performance for eukaryotic RNA-seq data. Alignment files in BAM format were generated for subsequent quantification analyses.

Gene expression quantification and batch effect correction

Gene-level raw read counts were obtained from the alignment BAM files using HTSeq-count based on the gene annotation file generated in this study. These raw counts were used as input for differential expression analysis.

In parallel, transcript assembly and expression estimation were performed using StringTie, and gene expression levels were calculated as fragments per kilobase of transcript per million mapped reads (FPKM). FPKM values were used for visualization purposes, including heatmap construction and expression pattern profiling.

For the gonadal developmental-stage dataset, potential batch effects resulting from differences in sequencing platforms and library preparation batches were corrected using the ComBat function in the sva R package. Batch correction was applied to normalized expression matrices for visualization analyses.

Differential expression and functional enrichment analysis

Differentially expressed genes (DEGs) were identified using the DESeq2 R package (version 4.2) [41]. DESeq2 performs internal normalization using size factors to account for library depth differences. Genes with $|\log_2$ fold change$| \geq 1$ and a Benjamini–Hochberg adjusted P-value (false discovery rate, FDR) < 0.05 were considered significantly differentially expressed.

Identified DEGs were subjected to Gene Ontology (GO) and Kyoto Encyclopedia of Genes and Genomes (KEGG) pathway enrichment analyses using the clusterProfiler R package. Enrichment significance was assessed using a hypergeometric test, and P-values were corrected using the Benjamini–Hochberg method.

Results

The sea urchin genome assembly and annotation

Genome sequencing of *S. intermedius* was performed using a combination of Illumina short-read sequencing (NovaSeq 6000 platform), PacBio long-read sequencing (Sequel II platform), and Hi-C sequencing technologies. Based on k-mer distribution, the genome size of *S. intermedius* was estimated, and the quality of the *S. intermedius* draft genome assembly was evaluated (Supplementary Table 1). The results showed that 97.56% of clean reads were mapped to our assembly. Among the 303 core eukaryotic genes, 274 (90.43%) were identified in the *S. intermedius* assembly. Subsequently, we obtained 115.94 Gb of high-quality sequencing data (164.47 × coverage) from long-read libraries using the PacBio Sequel II platform. We assembled a 704.9 Mb genome with contig N50 length of 1.5 Mb (Supplementary Table 2). Finally, we constructed Hi-C fragment libraries ranging from 300 to 700 bp insert size and 111.68 Gb (158.44 × coverage) data (Table 1) were generated through Illumina platform. Through analysis, a total

of 67,710,831 valid interaction pairs (58.9% of uniquely mapped paired-end reads) were generated from the Hi-C library. The valid interaction pairs were used for correction of scaffolds and clustered, ordered and orientated scaffolds onto chromosomes and 1,304 scaffolds (representing 97.77% total length) were anchored to 21 chromosomes (Fig. 1B, and Fig. 1C, and Supplementary Table 3). The final corrected *S. intermedius* genome size was 704.9 Mb with contig and scaffold N50 values of 1.5 Mb and 30 Mb (Fig. 1D). BUSCO analysis based on the *metazoa*_odb10 dataset identified 91.72% complete BUSCOs, including 89.62% single-copy and 2.10% duplicated BUSCOs, with only 0.63% fragmented and 7.65% missing BUSCOs. This indicated that the genome assembly was relatively complete, exhibited a low proportion of duplicated genes, and demonstrated high reliability (Fig. 1E). We uploaded the complete genomic data to NCBI (Bioproject ID: JBGVUB000000000, https://submit.ncbi.nlm.nih.gov/subs/wgs/SUB14698394/overview). These results confirmed that we successfully assembled a high-quality *S. intermedius* genome.

A total of 297.33 Mb of repetitive elements were identified, accounting for 42.18% of the *S. intermedius* genome. The repeats were dominated by LARDs (13.89%), LINEs (9.85%) and TIRs (8.12%) (Supplementary Table 4). In total, we successfully predicted 23,127 protein-coding genes by combining de novo prediction, homology-based prediction and transcriptome-based prediction methods. The average length of genes was 13,741 bp, of exons was 2,334 bp, and of introns was 11,406 bp (Fig. 1F). 14 microRNA, 239 ribosomal RNA, 1,684 transfer RNA and 1,039 pseudogenes in our genome were predicted. And 22,188 genes (95.94%) were functionally annotated in the *S. intermedius* genome by aligning protein-coding genes (Supplementary Table 5).

Comparative genomics reveals the phylogenetic position of*S. intermedius*, the expansion and contraction of gene families.

To understand the phylogenetic position of sea urchins, we performed a genome-wide phylogenetic analysis using the maximum likelihood method, which is based on single-copy genes from 11 genomes. Results from

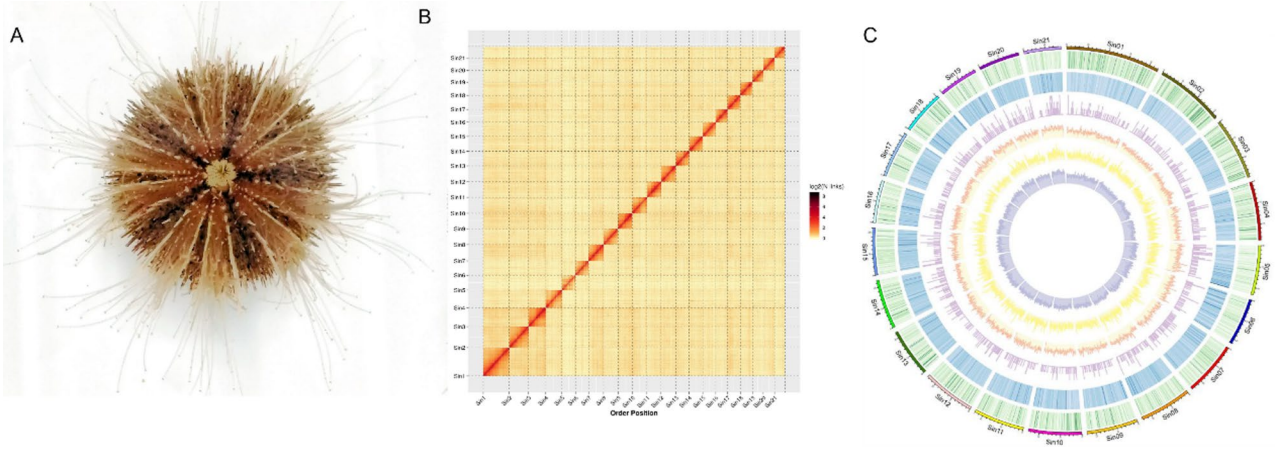

D

Assembly feature	Value
Scaffold number	1,340
Scaffold length (Mb)	704.9
Scaffold N50 (Mb)	30
Contig number	1,912
Contig length (Mb)	704,9
Contig N50 (Mb)	1.5
GC content (%)	37.5

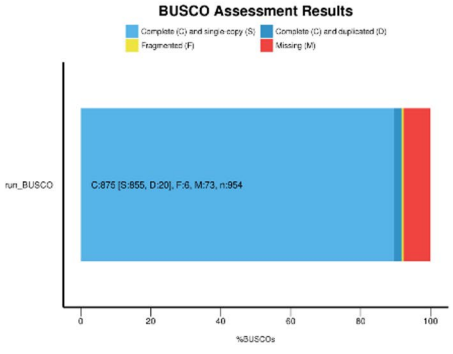

F

Feature	Value
Gene Num	23,127
Gene length (bp)	317,781,811
Ave Gen length (bp)	13,740.73
Exon length (bp)	53,986,439
Ave Exon length (bp)	2,334.35
Exon Num	178,792
Ave exons per gene	7.73
Intron length (bp)	263,795,372
Ave Intron length (bp)	11,406.38
Intron Num	155,665
Ave Introns per gene	6.73

Fig. 1 Chromosome-level genome assembly of S. intermedius. **A***S. intermedius*. **B** Interactive thermography of Hi-C assembly chromosomes. **C** A schematic representation of the genomic characteristics of *S. intermedius*. From outside to inside: 1. miRNA distribution location, 2. chromosome, 3. repeat sequence distribution, 4. gene distribution. they are sliding window 500k. **D** Statistics for the final corrected *S. intermedius* genome. **E** BUSCO assessment results of the *S. intermedius* genome assembly completeness. **F** Summary of predicted genes

the phylogeny and fossil record indicate that chordates diverged from echinoderms approximately 669 million years ago (Mya). This divergence roughly coincides with the Lower Cambrian Evolutionary Orogeny. In addition, evolutionary analyses of 8 echinoderms (*A. japonicus*, *P. miniata*, *A. planci*, *A. japonica*, *L. variegatus*, *L. pictus*, *S. purpuratus*, and *S. intermedius*) indicate that sea urchins are the sister group to sea cucumbers and are estimated to have diverged about 574 Mya, suggesting that the 5 echinoderm classes have had a lengthy evolutionary history after divergence. Meanwhile, we found that *S. intermedius* and *S. purpuratus* diverged from their common ancestor ~31 million years ago (Fig. 2A). The protein sequences of *S. intermedius* and 10 other species were employed for gene family clustering, resulting in a total of 133,856 gene families. (Fig. 2B, Supplementary Table 6). A total of 132 gene families were unique to *S. intermedius*, 14,494 orthologs were identified for *S. intermedius*, which could cluster with the other 9 species. Across the four sea urchin species, we identified a total of 10,837 shared gene families (Fig. 2C).

To further assess lineage-specific gene family dynamics in *S. intermedius*, we compared gene family sizes with those inferred for the most recent common ancestor. A total of 1,150 gene families showed significant expansion and 1,894 showed significant contraction ($P < 0.05$). GO enrichment analysis of significantly expanded gene families showed enrichment in receptor activity, molecular transducer activity, and transmembrane signaling receptor activity (Fig. 3A). KEGG enrichment indicated significant representation in Neuroactive ligand-receptor interaction, Calcium signaling pathway, and cAMP signaling pathway (Fig. 3B). Interestingly, we found an expansion of the *Elovl* gene family associated with fatty acid synthesis. Meanwhile, the 12 *Elovl* genes were sequenced and a phylogenetic tree was constructed, and

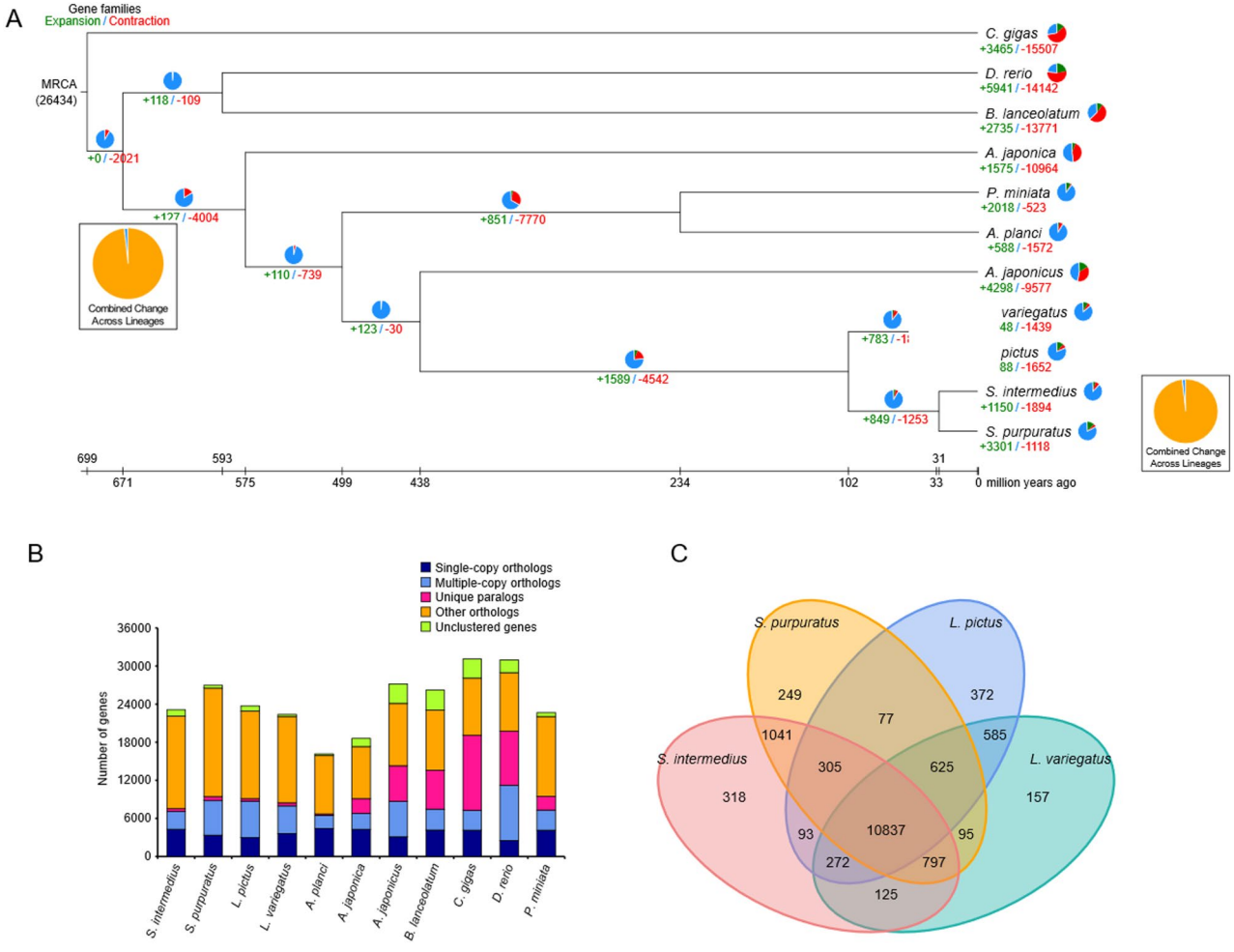

Fig. 2 Comparative genomic analysis between *S. intermedius* and others. **A** Phylogenetic placement of *S. intermedius* within the metazoan tree. The numbers on the branches indicate the number of gene gains (+) and the number of gene losses (–), which are also displayed as bar plots: gene gain (in green), gene loss (in red), and the remaining gene families (in blue). The divergence times were estimated and displayed below the phylogenetic tree. **B** Comparison of the gene repertoire of 11 metazoan genomes. **C** The shared and unique gene families in 4 species of Echinoidea are shown in the Venn diagram

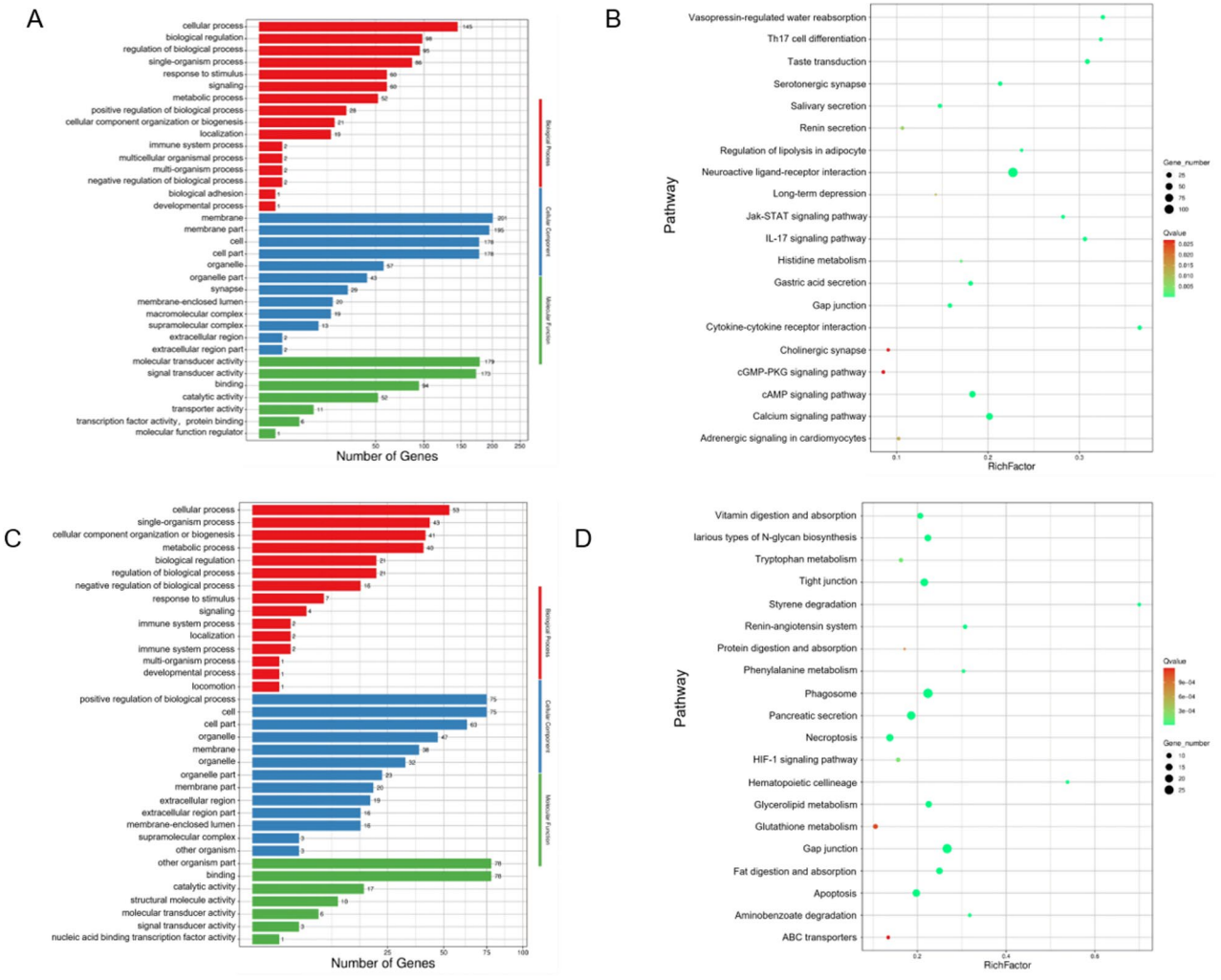

Fig. 3 Functional enrichment analysis (GO and KEGG) of expanded and contracted gene families. **A** GO enrichment analysis of significantly expanded gene families. **B** KEGG pathway enrichment analysis of significantly expanded gene families. **C** GO enrichment analysis of significantly contracted gene families. **D** KEGG enrichment analyses of the significantly contracted gene families

the results are shown in Fig. 4 and Supplementary Table 7. In addition, we also found that genes from the contraction-related gene family were significantly enriched in phagocytosis, apoptosis, HIF-1 signaling, and glutathione metabolism (Fig. 3C-D). We identified 33 *GST* genes and constructed a phylogenetic tree.

Based on the hypothesis that the rapidly evolving genes have been under positive selection, we identified 418 positively selected genes (PSGs) using the codeml model (F3 × 4 model of codon frequencies) in PAML. These PSGs were considered to be involved in the functional categories of "structural constituent of ribosome", "threonine-type endopeptidase activity", "threonine-type peptidase activity", etc. These PSGs were significantly enriched in the "Proteasome (ko03050)" and "Ribosome (ko03010)" pathways (Supplementary Table 7). The specific and expanded gene families and PSGs in *S. intermedius* suggest that fatty acid synthesis and adaptive evolution to the harsh environment occurred at the genomic level.

Transcriptomes at gonad development stages of *S. intermedius*

Gonadal growth and development is a complex process involving a large number of genes (NCBI BioProject ID: PRJNA1200219), and the corresponding sequence data are presented in Fig. 5 and Supplementary Tables 8 and 9. To investigate fatty acid biosynthesis and metabolism during the sea urchin gonadal development, we performed transcriptomic comparisons across four developmental stages in both females and males (Ost1–Ost4 for ovaries; Tst1–Tst4 for testes). Differential expression analysis was conducted using pairwise contrasts among all gonad developmental stages within each sex. Specifically, the data from each stage were compared with the pooled data from the other three stages, and the details

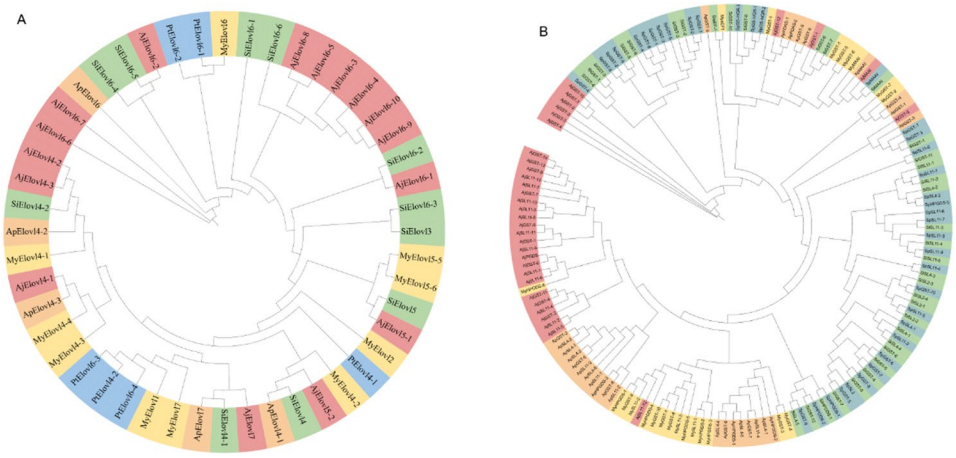

Fig. 4 Phylogenetic relationship of Elovl (**A**) and GST (**B**) genes between *S. intermedius* and related species. The green branch indicates the *S. intermedius* lineage that underwent a significant expansion of the Elovl gene family or contraction of the GST gene family

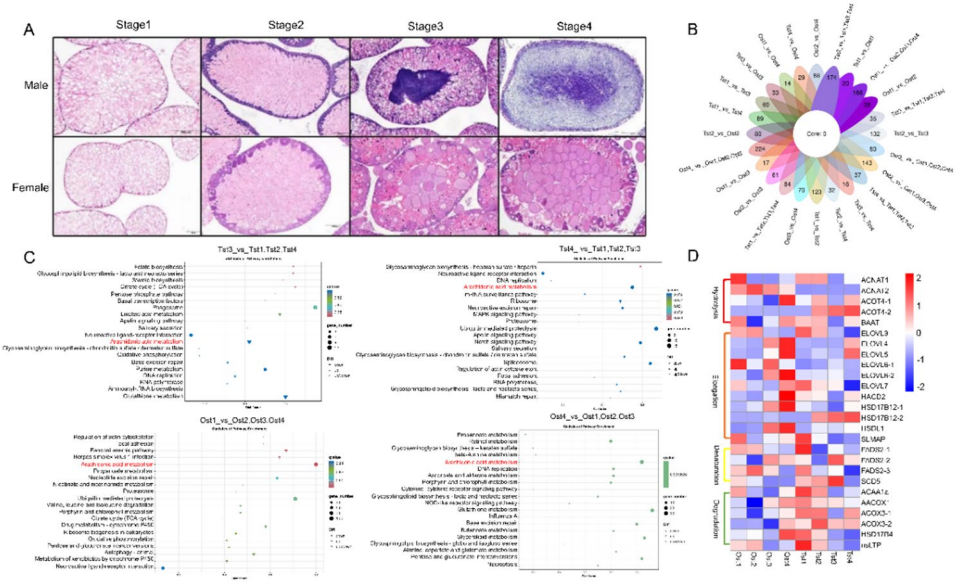

Fig. 5 Fatty acid synthesis-related pathways and gene expression during gonadal development in sea urchins *S. intermedius*. **A** Histological features of the sea urchin *S. intermedius* gonads at different gonad development stages. Paraffin-embedded sections were stained with hematoxylin and eosin. Scale bar: 100 μm. Stage 4 gonads (Ost4, female; Tst4, male) were newly prepared for this study. Samples Ost1–Ost3 and Tst1–Tst3 were derived from our previously published data (PRJNA532998). **B** Venn diagram of DEGs in each comparison group

of the group comparisons were provided in Supplementary Tables 10 and 11.

In female sea urchins, 168, 143, 83, and 224 DEGs were identified when Ost1, Ost2, Ost3, and Ost4 were each compared with the pooled data from the other three stages, respectively. In male sea urchins, 84, 174, 35, and 37 DEGs were identified when Tst1, Tst2, Tst3, and Tst4 were compared with the pooled data from the other three stages, respectively (Fig. 5B).

To determine the functional categories associated with transcriptional changes during gonadal growth and development, KEGG enrichment analysis was performed. The top 20 KEGG pathways associated with sea urchin gonadal development are presented in Fig. 5C and Supplementary Table 12. The most common metabolic pathways were: neuroactive ligand-receptor interaction, arachidonic acid metabolism, nucleotide excision repair, ubiquitin mediated proteolysis, base excision repair and RNA polymerase.

Among the top 20 KEGG pathways (Supplementary Table 8), the neuroactive ligand-receptor interaction pathway was found in all groups except for Ost4 group. In the other KEGG analysis, nucleotide excision repair pathway showed higher activity in Tst1, Ost1, Tst2, Ost3, and Tst4. During stage 1 and stage 2, ubiquitin mediated proteolysis pathway exhibited higher activity in both

sexes, including Tst4. Base excision repair pathway demonstrated greater activity in Tst1, Ost2, Tst3, and Ost4. Furthermore, RNA polymerase was found to be present in all teste's groups.

Among all KEGG pathways, those related to fatty acid metabolism were consistently active across all stages of gonadal development (Supplementary Table 13). The most active pathway in this category was the arachidonic acid metabolism pathway, which showed higher activity in most ovary development stages (Ost1, Ost2, and Ost4) as well as in the mature testis stages (Tst3 and Tst4). Specifically, during testis stage 4, there were 35 DEGs identified to be involved in arachidonic acid metabolism (Supplementary Table 9). Linoleic acid metabolism was found to be more active in Ost2 and Tst3. Additionally, fatty acid metabolism and biosynthesis pathways displayed significantly higher activity in Tst2 and Ost3, respectively.

Based on the identified DEGs, we further focused on the biosynthesis of unsaturated fatty acids (ko01040) which was present throughout gonad development, and this pathway included several key processes, such as elongation, desaturation, degradation, and hydrolysis (Supplementary Table 14). This metabolic pathway detailed the various reactions involved in the synthesis and modification of unsaturated fatty acids, with a particular emphasis on n-3 and n-6 polyunsaturated fatty acids (PUFAs), which were our primary focus (Supplementary Fig. 1). As the two major PUFAs, EPA (n-3) and ARA (n-6) reached their highest concentrations at stage 2 of gonadal development [5], suggesting that the unsaturated fatty acid biosynthesis pathway was more active at this stage than at others. In male sea urchins, the unsaturated fatty acids biosynthesis pathway was more active at stage 1, where all four processes were present. In female sea urchins, all four processes were present at stage 2, and the pathway was most active at this stage (Supplementary Table 15). In other stages, only some of the processes were included, not all of them. For example, there was only one DEG in desaturation process at growth stage of testis (Tst2).

In the hydrolysis process within this pathway, the genes encoding peroxisomal succinyl-coenzyme A thioesterase (*ACOT4-1*) and acyl-coenzyme A thioesterase 4 (*ACOT4-2*) exhibited higher expression in the ovary and testis, respectively. *ACOT4-1* showed peak expression during the growth stage (stage 2), while *ACOT4-2* expression increased progressively with testis development (Fig. 5D). In the elongation process, there were six types of fatty acid elongation proteins (*Elovl*), and the expression of *Elovl6-1* decreased throughout gonad development. The gene expression levels of inactive hydroxysteroid dehydrogenase-like protein 1 (*HSDL1*) in the ovary and fatty acid elongation protein 3 (*Elovl 3*) in the testis increased with gonad development. *Elovl3* exhibited significantly higher expression in the testis compared to the ovary. There were three types of acyl-CoA 6-desaturases (*FADS*) and one stearoyl-CoA desaturase in the desaturation process. The gene expression level of *SCD5* was significantly higher than that of the other desaturases. In the degradation process, 3-ketoacyl-CoA thiolase A (peroxisomal-like, *ACAA1a*) showed higher expression than other enzymes in both sexes of gonads. The gene expression of peroxisomal multifunctional enzyme type 2-like (*HSD17B4*) and non-specific lipid-transfer protein (*nsLTP*) decreased with testis development (Fig. 5D and Supplementary Table 16).

Transcriptomic profiling during larval development in the *S. intermedius*

To investigate metabolic remodeling associated with metamorphosis and the larval-to-benthic dietary transition, the transcriptome of *S. intermedius* was profiled across 15 developmental stages (45 samples; Fig. 6A). Sequencing statistics are listed in Supplementary Table 17; raw data are available under PRJNA1199686.

A total of 45 samples from different developmental periods of *S. intermedius* were divided into 15 groups. All the differential expression genes statistics are shown in (Fig. 6B, Supplementary Table 18). KEGG enrichment analysis of DEGs from FE to JSU revealed significant pathway enrichments at each developmental stage (Fig. 6C, Supplementary Table 19).

During early embryonic development (fertilized egg to 32-cell stage), DEGs were enriched in DNA replication and RNA transport pathways, reflecting rapid cell proliferation and early developmental programming. Notably, pathways related to fatty acid metabolism, *FoxO* signaling, *Notch* signaling, and pyruvate metabolism were also detected. In the planktonic larval stage (gastrula to 8-armed larva), DEGs differing between the gastrula and blastula stages were significantly enriched in the lysosome pathway (q-value < 0.05). During the long-armed larval stage, DEGs were significantly enriched in pathways including inositol phosphate metabolism, steroid biosynthesis, biosynthesis of unsaturated fatty acids, and arachidonic acid metabolism. In the metamorphic attachment stage, DEGs in sea urchins were significantly enriched in pathways related to arginine and proline metabolism, phosphatidylinositol signaling system, ECM-receptor interaction, glycosaminoglycan biosynthesis (chondroitin sulfate/dermatan sulfate) (Fig. 6C).

Genes involved in fatty acid synthesis, elongation, and activation exhibited coordinated developmental regulation (Fig. 6D). Overall, multiple genes associated with de novo fatty acid synthesis and elongation showed higher expression during embryonic and early larval stages and progressively decreased toward later larval and juvenile

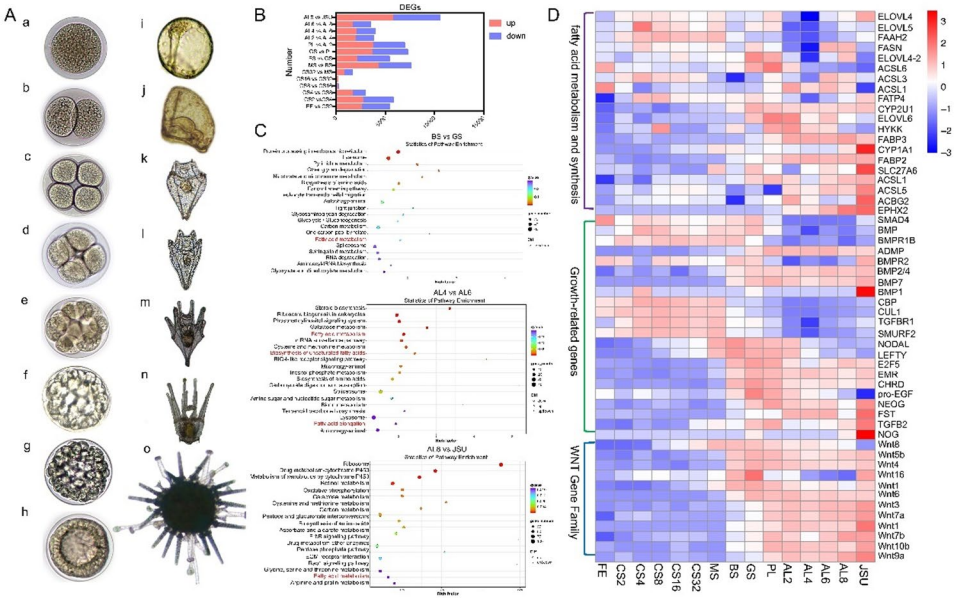

Fig. 6 Screening and functional analysis of key genes in *S. intermedius* at different developmental periods. **A** Different development stage of *S. intermedius*. a: fertilized egg (FE), b: 2 cell stage (CS-2), c: 4 cell stage (CS-4), d: 8 cell stage (CS-8), e: 16 cell stage (CS-16), f: 32 cell stage (CS-32), g: multicellular stage (MS), h: blastula stage (BS), i: gastrula stage (GS), j: prism larvae (PL), k: 2-armed larvae (AL-2), l: 4-armed larvae (AL-4), m: 6-armed larvae (AL-6), n: 8-armed larvae (AL-8), o: juvenile sea urchin (JSU). **B** The number of DEGs in each comparison group, red represents up-regulated genes, and blue represents down-regulated genes. **C** KEGG enrichment analysis of DEGs at key developmental stages (BS vs GS, AL4 vs AL6, and AL8 vs JSU) in *S. intermedius***D** Heatmap of key gene expression for growth and development and fatty acid synthesis

stages. Long-chain-fatty-acid-CoA ligase 1 (*ACSL1*) showed the highest expression at the FE and CS. Fatty acid synthase, elongase *Elovl4*, *ACSL6*, *CYP2U1*, and *Elovl6* reached peak expression from GS–AL. In contrast, *Elovl5* and *ACSL3* exhibited relatively higher expression in JSU. Several lipid transport and processing genes, including *Elovl4*, fatty acid-binding protein 2 (*FABP2*), *ACSL1*, *ACSL5*, *ACSBG2*, soluble epoxide hydrolase-like protein 2 (*sEH2*) were highest expressed in JSU (Fig. 6D).

In addition, key genes involved in bone and body axis formation—including calmodulin (*CALM*), *Hox*, *Wnt*, and *TGF-β* superfamily members—exhibited stage-specific expression patterns. *CALM* and calcium-binding genes were highly upregulated after the prism larval stage (PL), while multiple *Hox* genes showed peak expression at specific stages such as blastula (BS) and gastrula (GS). Members of the *Wnt* and *TGF-β* families (e.g., *BMP*, *Wnt8*, *Wnt3*) also displayed distinct expression maxima across early developmental stages, including the multicellular (MS), gastrula (GS), and juvenile sea urchin (JSU) stages (Supplementary Table 20).

Dicussion

Genome assembly and evolutionary analysis of *S. intermedius*

In the field of sea urchin genomics, the genome of the purple sea urchin (*S. purpuratus*) was sequenced in 2006. This assembly, approximately 814 Mb in length and encoding around 23,300 genes, revealed that sea urchins and other echinoderms share a closer phylogenetic affinity with humans and other chordates than previously recognized [42, 43]. Subsequently, the genome sequences of several other sea urchin species have been reported, including *Hemicentrotus pulcherrimus* [44], *L. variegatus* [45], *Paracentrotus lividus* [46], *Mesocentrotus franciscanus* [47], and *Anthocidaris crassispina* [48]. In this study, we sequenced and assembled the whole genome of *S. intermedius*. The assembled genome had 21 chromosomes, with a total length of 704.9 Mb, a scaffold N50 of 30 Mb, and encodes 23,127 genes. In the previous study, we performed a karyotype analysis of *S. intermedius* and determined that a diploid chromosome number of 2n = 42 (2n = 20 m + 20sm + 2st) [49]. Furthermore, we revealed that sea urchins within the family Strongylocentrotidae (*S. intermedius*, *H. pulcherrimus*, and *M. franciscanus*) and the family Echinometridae (*A. crassispina*) all possess 21 chromosomes [50]. Significantly, ancestral sea urchin lineages (e.g., genera Arbacia and Stomopneustes) typically possess 22 chromosomes . This indicates that *S. intermedius* and related species within the Strongylocentrotidae have undergone a chromosomal fusion event during their evolution.

Compared with other published echinoid genomes, the total span of the *S. intermedius* assembly falls at the lower end of the reported genome size range. Nonetheless, the final assembly size is consistent with the present genome survey estimation. It is also supported by strong short-read mapping, Hi-C scaffolding consistency,

and high BUSCO completeness. These results indicate that the assembly is unlikely to reflect large-scale collapse or systematic loss of conserved genes. In several other sea urchin assemblies, repetitive elements constitute a considerable fraction of the genome. For example, repetitive sequences account for approximately 39.6% of the assembly of *Echinometra lucunter* [51]. In addition, repetitive regions comprise about 45.4% of the *L. variegatus* genome [52]. These findings indicate that repetitive sequences are a major component of echinoid genome architecture. Variation in repeat content and other noncoding components may therefore contribute to differences in total genome span among closely related species. In our study, the predicted number of protein-coding genes in *S. intermedius* is comparable to that reported for other sea urchins. This suggests that genome size differences among these species are unlikely to be primarily driven by changes in coding gene content. This foundational work establishes a framework for subsequent comparative genomic analyses within echinoderms.

Beyond providing a high-quality genomic resource, the assembled genome also enables the investigation of gene family evolution associated with key traits in *S. intermedius*. Notably, genes involved in fatty acid biosynthesis showed significant expansion. In our previous study, we first performed lipidomics profiling of lipid abundances in *S. intermedius* and detected 11 polyunsaturated fatty acids in the sea urchin gonads, accounting for 54.13% of the total fatty acid content, and also identified polyunsaturated fatty acid (42:11) as a potential marker to distinguish high levels of polyunsaturated fatty acids in individual sea urchins [53]. We clarified the relationship between sea urchin gonadal development and fatty acid synthesis metabolism, proving that intermediate sea urchins have the ability to synthesize fatty acids endogenously [4]. Secondly, we sequenced the gonadal transcriptomes of both sexes at various developmental stages of *S. intermedius*, identifying critical genes related to gonadal growth as well as fatty acid biosynthesis and metabolism [4]. We have focused on the PUFA biosynthesis pathway, specifically the genes involved in fatty acid desaturase (*SiFad1*, *Δ6Fad-like*, *Fad2*) and elongase of long chain fatty acids (*Elovl4-like*, *Elovel5-like*) gene families [8, 54, 55]. Interestingly, in this study, the expanded gene families were mainly enriched for fatty acid elongation, biosynthesis of unsaturated fatty acids and fatty acid metabolism ($P < 0.05$). We found the expansion of elongase of long chain fatty acids family 6 (*ELOVL6*). As known, *ELOVL6* is an enzyme that specifically catalyzes the elongation of saturated and monounsaturated fatty acids with 12, 14 and 16 carbons [56]. These findings may be related to the fatty acid rich gonads of *S. intermedius*, further confirms the endogenous synthesis of fatty acids in *S. intermedius* [57, 58].

This expansion is likely an adaptive evolutionary response to its dietary niche and reproductive demands. As sea urchins primarily feed on macroalgae, which are rich in C18 precursors like α-linolenic acid (ALA) but poor in longer-chain PUFAs such as EPA and DHA, the enhanced elongation capacity provided by additional *Elovl* genes enables the efficient conversion of dietary short-chain PUFAs into biologically critical long-chain PUFAs (LC-PUFAs). The functional implications of this genetic expansion are profound [59]. LC-PUFAs serve as essential components of phospholipids in cellular membranes, particularly in gonadal and neural tissues, where they maintain membrane fluidity and facilitate signal transduction [60]. Moreover, they act as precursors for signaling molecules such as eicosanoids, which regulate reproduction and immune responses [61]. The observed gene family expansion likely enhances the organism's ability to accumulate lipids in gonads, thereby improving gamete quality and larval viability [62]. This genetic adaptation not only underscores the evolutionary strategy of *S. intermedius* to thrive in its environment but also provides a molecular foundation for its high nutritional value. Consequently, these findings offer critical insights into the genetic mechanisms underlying PUFA biosynthesis in marine invertebrates and highlight potential targets for selective breeding aimed at enhancing lipid profiles in aquaculture species.

In addition, we identified a contraction of the *GST* gene family in sea urchins, which may reflect reduced chemical or oxidative stress in their specific ecological environment. This contraction may be associated with reduced detoxification capacity, which could affect survival and reproductive success. It also suggests that GST gene family evolution in *S. intermedius* may be linked to ecological adaptation.

Dynamic changes of fatty acid biosynthesis and metabolism during gonadal development of *S. intermedius*

The processes of gonad growth and development are intricate biochemical pathways that involve multiple gene expression networks, accompanied by fatty acid biosynthesis and metabolism during the gonad development. In this study, we focused on the primary four developmental stages of sea urchin gonads, which are the active periods of nutrient enrichment as well as fatty acid biosynthesis and metabolism, and explored the differences in fatty acid synthesis and metabolism between male and female sea urchin gonads.

Patterns of fatty acid biosynthesis and metabolism during gonad development

Our results showed that fatty acid metabolism and the biosynthesis of unsaturated fatty acids remained active throughout gonadal maturation in *S. intermedius*. This

indicates active lipid metabolism during reproductive development, supported by both algal dietary input and intrinsic physiological demands [5]. According to our previous study, the concentration of PUFAs—particularly EPA and ARA—was significantly higher than that of SFAs and MUFAs at stage 2 in both sexes [8]. Combined with the transcriptomic evidence presented here, these findings suggest that long-chain PUFAs are continuously involved in gonadal development rather than being transiently accumulated at specific stages. As major components of membrane phospholipids, PUFAs contribute to membrane fluidity, permeability, and protein activity, which may be particularly important for gamete development and fertilization [63]. In addition, ARA and EPA can serve as precursors for bioactive molecules involved in reproduction, immunity, and inflammation, thereby supporting gonadal development and physiological homeostasis [64, 65]. The high levels of EPA and ARA during gonadal development are therefore linked to energy demand, gametogenesis, and signaling molecule synthesis. Gonadal development requires substantial energy, and fatty acids serve as crucial energy reserves supporting cell division and growth [66, 67].

Notably, ARA metabolism remained highly active across gonadal development, especially during most ovarian stages and in mature testes, highlighting its potential importance in reproductive regulation. Sea urchin gonads are notably rich in ARA [4, 53, 68, 69], which has been shown to improve oocyte development and maturation, as demonstrated in swamp eel [70]. In our previous dietary study, higher ARA levels (1% dry diet) promoted growth, gonad development, antioxidant enzyme activity, and nutritional quality in adult sea urchins [71]. Taken together, these observations indicate that ARA serves as a stored lipid component and a metabolically active molecule that contributes to gonadal maturation and function. In particular, ARA is associated with oocyte maturation, fertilization, and embryonic development in sea urchins and other invertebrates [62, 72]. Additionally, in cold-water species such as *S. intermedius*, high PUFA levels help maintain membrane fluidity at low temperatures, preventing rigidification and supporting environmental adaptation [73]. Thus, continuous fatty acid biosynthesis and metabolism are essential for sea urchin reproduction and development, providing both flexible energy reserves and structural and signaling molecules necessary for successful maturation and breeding.

Gender differences in unsaturated fatty acid biosynthesis

From the first stage of gonadal development, when primary spermatocytes and oocytes are just differentiated, the fatty acid biosynthesis pathways become active in sea urchin gonads, preparing for gamete formation. From an evolutionary perspective, testes develop earlier than ovaries, which is primarily related to reproductive strategies and energy allocation. Our previous study found that testis development progresses 1–2 months faster than ovary development [5]. When gonad development is at the same stage, there are also differences in fatty acid biosynthesis and metabolism between testis and ovary. During testis development, fatty acid synthesis and metabolism are most active at stage 1, especially the biosynthesis of unsaturated fatty acids (10/39). In the ovary, fatty acid synthesis and metabolism are relatively active during the throughout gonad development. In males, fatty acid biosynthesis activity is concentrated in stage 1 to prepare for rapid sperm production (spermiation occurs earlier than ovulation). In females, increased energy and fatty acids are required for oocyte production and early embryonic development. Accordingly, fatty acid synthesis and metabolism remain active throughout gonadal development, becoming more pronounced from stage 2, as reflected by the peak expression of the *ACOT4-1* gene observed at this stage in the present study. Early-maturing male sea urchins can participate in mating earlier during the breeding season, increasing their chances of encountering females and thereby improving reproductive success [74, 75]. Moreover, male sea urchins produce a relatively large quantity of sperm, which they can release to ensure successful fertilization. In contrast, female sea urchins need more energy for egg production and subsequent reproductive behaviors. Thus, early maturation in males allows them to better adapt to environmental changes and competition, enhancing the reproductive efficiency of the population [76].

The molecular mechanisms of fatty acid synthesis and metabolism during the embryonic and larval development of*S. intermedius*.

Gradual decrease of endogenous nutrients during S. intermedius individual development

Early studies reported a decline in total lipid content from the swimming blastula to pluteus stage in sea urchins, primarily due to triglyceride consumption [6, 77]. This indicates a shift from maternal lipid utilization to exogenous energy acquisition during early development [77]. Consistent with these physiological observations, our transcriptomic data revealed a progressive downregulation of key genes involved in fatty acid biosynthesis and elongation, including *Elovl4*, *Elovl5*, and *FASN*, from embryonic to larval stages. These expression patterns indicate that the capacity for de novo fatty acid synthesis gradually declines during development, suggesting that early larvae primarily rely on maternally deposited lipid reserves to support growth and morphogenesis [54]. Compared with previous studies focusing mainly on lipid consumption at the biochemical level, the

present results provide transcriptomic evidence linking endogenous lipid utilization with the coordinated expression of fatty acid metabolic genes in *S. intermedius*. During early larval stages, such as the echinopluteus stage, these stored lipids are progressively mobilized to support larval development, further emphasizing the important role of maternal lipid reserves in early developmental stages. Such transcriptional suppression likely promotes the utilization of stored lipids to support development until exogenous feeding begins.

The developmental transition toward nutritional independence is accompanied by metabolic reprogramming. During the echinopluteus stage, larvae show enrichment of pathways for energy production [78], synthesizing lipids primarily from dietary sources rather than endogenous pathways [79]. This strategy optimizes energy allocation, reserving maternal reserves for critical developmental processes.

Time-series developmental transcriptome studies in other sea urchins have shown that development proceeds through relatively stable gene-expression states punctuated by discrete transitions, reflecting broad transcriptional reprogramming coupled to major physiological and metabolic shifts [80, 81]. In this context, our study observed the gradual downregulation of fatty acid synthesis and elongation genes, which reflects a transcriptional signature of metabolic reprogramming during development. Combined with the developmental shift from maternal provisioning toward nutritional independence, these expression patterns support a parsimonious metabolic interpretation: early embryos/larvae increasingly depend on maternally supplied lipid reserves, whereas later stages reduce endogenous synthesis and become more reliant on exogenous nutrient inputs. This change in lipid metabolism regulation in *S. intermedius*, particularly the downregulation of fatty acid synthesis, may not simply be a passive consequence of nutrient depletion, but rather a tightly regulated developmental process. These findings highlight the regulation of lipid metabolism during the early development of *S. intermedius*, offering a new perspective on the metabolic transitions that occur during sea urchin development.

Preliminary exploration of the molecular mechanism of dietary shift during S. intermedius metamorphosis

Changes in life history and diet play a key role in physiological adaptation, as evidenced by the regulation of multiple signalling pathways and metabolic processes. The transition of sea urchins from planktonic to benthic larvae is a complex biological process involving the regulation of multiple signalling pathways and metabolic processes, which is specific to indirect-developing urchins [82, 83]. In this context, the differential gene expression patterns suggest that metamorphosis in *S. intermedius* is not only a morphological transition, but also a coordinated metabolic transition associated with dietary shift. During the planktonic larval stage, their primary food source is unicellular planktonic algae, whereas after metamorphosis and settlement, their diet primarily consists of benthic diatoms and other marine plants. Benthic diatoms are rich in extracellular polysaccharides, amino acids, and unsaturated fatty acids [84]. These unsaturated fatty acids provide essential lipids for membrane biogenesis and energy metabolism. As their diet changes, sea urchins gradually reduce endogenous fatty acid synthesis and instead prioritize the utilization of exogenous fatty acids. In our study, during the juvenile stage, the expression of genes related to fatty acid synthesis significantly decreased, such as *Elovls* genes, *Fasn*, and *Acsls*, with some genes showing extremely low expression levels. This pattern suggests that, during the transition to a benthic lifestyle, sea urchins reduce endogenous fatty acid synthesis and increasingly depend on exogenous nutrient sources, reflecting a metabolic shift at the transcriptomic level. These results suggest that the dietary transition during sea urchin metamorphosis is accompanied by coordinated adjustment of lipid utilization. Such regulation may help juveniles better exploit nutrient resources in the benthic habitat to support subsequent growth and development [85, 86].

Transcriptome analysis revealed that DEGs of the metamorphic attachment stage were significantly enriched in ECM-receptor interaction, *Hox*, and *Wnt* pathways. These pathways are closely associated with attachment, body-plan remodeling, and benthic adaptation, suggesting that the larval-to-benthic transition involves broader developmental reprogramming rather than an isolated nutritional change. Combined with the concurrent changes in fatty acid metabolism-related genes, our results may indicate coordinated structural and metabolic adjustments during *S. intermedius* metamorphosis, potentially contributing to ecological adaptation in the benthic environment [87–89].

Conclusions

We assembled a chromosome-level genome of *S. intermedius* with a total size of 704.9 Mb and a scaffold N50 of 30 Mb. Comparative genomic analysis showed an expansion of the *Elovl* gene family, suggesting an enhanced capacity for fatty acid synthesis in this species.

In terms of gonadal development, unsaturated fatty acid biosynthesis remains consistently active at all stages, with the arachidonic acid (ARA) metabolism pathway showing height active during ovarian development (stage 1–4) and mature testis stages (stage 4). Notable gender differences are observed in unsaturated fatty acid biosynthesis: females exhibit sustained active of biosynthesis, especially during ovary maturity to prepare for embryo

development, while males primarily focus on biosynthesis during the immature testis stage to ensure rapid sperm production ahead of ovulation. These reproductive strategies enhance the propagation and survival of sea urchin populations.

During the embryonic and larval development of *S. intermedius*, the expression of *Elovl* genes gradually decreases, reaching nearly undetectable levels by the four-armed larval stage. This suggests that endogenous lipid reserves are gradually consumed during development.

In summary, we obtained a chromosome-level genome of sea urchin *S. intermedius*, elucidated its evolutionary relationships, demonstrated the endogenous synthesis of fatty acids, and provided valuable insights into the regulation of fatty acid synthesis and metabolism.

Supplementary Information

The online version contains supplementary material available at https://doi.org/10.1186/s12864-026-12764-1.

Supplementary Material 1.

Supplementary Material 2.

Authors' contributions

Lingshu Han: Investigation, Data curation, Formal analysis, Writing – original draft, Writing – review & editing. Jun Ding: Conceptualization, Methodology, Project administration, Funding acquisition, Supervision, Writing – review & editing. Heng Wang: Investigation, Data curation, Formal analysis, Writing – original draft. Yang Zhang: Investigation, Data curation. Junxiao Sun: Resources. Chong Zhao: Resources, Writing – review & editing. Weijie Zhang: Resources. Rantao Zuo: Resources. Wenpei Wang: Investigation, Data curation. Ye Tian: Investigation, Data curation. Yaqing Chang: Conceptualization, Project administration, Funding acquisition, Supervision, Writing – review & editing.

Funding

This research is supported by the National Natural Science Foundation of China (Project No.: 32373109), the Major Agricultural Project of the Liaoning Provincial Science and Technology Department (Project No.: 2023JH1/10200007), Liaoning Province "Xingliao Talents Plan" project (Project No.: XLYC2202001), the National Key Research and Development Program of China (Project No.: 2018YFD0901600).

Data availability

The original contributions presented in the study are included in the article/Supplementary Material. Further inquiries can be directed to the corresponding authors. The sequencing data that support the findings of this study are openly available in the NCBI: the whole-genome assembly of the sea urchin (*Strongylecentrotus intermedius*) has been submitted to GenBank under the accession number JBGVUB000000000 and BioProject ID: PRJNA1154782. The RNA-seq reads have been submitted to the NCBI SRA database (BioProject ID: PRJNA532998, PRJNA1200219 and PRJNA1199686).

Declarations

Ethics approval and consent to participate

The sea urchin *S. intermedius* is neither an endangered nor protected species. All experiments in this study were conducted according to national and institutional guidelines.

Consent for publication

Not applicable.

Competing interests

The authors declare no competing interests.

Author details

[1]Key Laboratory of Mariculture & Stock Enhancement in North China's Sea, Ministry of Agriculture and Rural Affairs, Dalian Ocean University, No. 52, Heishijiao Street, Shahekou District, Dalian, Liaoning 116023, PR China
[2]Key Laboratory of Northern Aquatic Germplasm Resources and Genetic Breeding in Liaoning Province, Dalian Ocean University, Dalian 116023, PR China
[3]Liaoning Province Aquatic Germplasm Resources Protection and Utilization Engineering Research Center, Dalian Ocean University, Dalian, Liaoning 116023, PR China

Received: 10 October 2025 / Accepted: 13 March 2026
Published online: 24 March 2026

References

1. Ding J, Chang Y. Research progress in conservation and utilization of economic echinoderm: a review. J Dalian Ocean Univ. 2020;35:645–56. https://doi.org/10.16535/j.cnki.dlhyxb.2020-157.
2. Zhenhui L, Li XZ, Xinyi. The research progress on the role of fatty acids in gonadal formation,gametogenesis and embryonic development. Volume 53. PERIODICAL OF OCEAN UNIVERSITY OF CHINA; 2023. pp. 1–9.
3. Li L, Yang D, Zuo R, Wang H, Ding J, Chang Y. Changes in lipids and fatty acids in gonads of sea urchin Strongylocentrotus intermedius before and after reproduction. J Dalian Ocean Univ. 2018;33:423–9. https://doi.org/10.16535/j.cnki.dlhyxb.2018.04.002.
4. Wang H, Ding J, Ding S, Chang Y. Transcriptome analysis to characterize the genes related to gonad growth and fatty acid metabolism in the sea urchin *Strongylocentrotus intermedius*. Genes Genomics. 2019;41:1397–415. https://doi.org/10.1007/s13258-019-00864-0.
5. Wang H, Zhao W, Liu X, Gang D, Zuo R, Han L, Chang Y, Ding J. Comparative Lipidome and Transcriptome Provide Novel Insight Into Polyunsaturated Fatty Acids Metabolism of the Sea Urchin. Front Mar Sci. 2022;9:777341. https://doi.org/10.3389/fmars.2022.777341.
6. Sewell MA. Utilization of lipids during early development of the sea urchin Evechinus chloroticus. Mar Ecol Prog Ser. 2005. https://doi.org/10.3354/meps304133.
7. Byrne M, Prowse T, Sewell M, Dworjanyn S, Williamson J, Vaïtilingon D. Maternal provisioning for larvae and larval provisioning for juveniles in the toxopneustid sea urchin Tripneustes gratilla. Mar Biol. 2008;155:473–82.
8. Wang H, Ding J, Ding S, Chang Y. Integrated metabolomic and transcriptomic analyses identify critical genes in eicosapentaenoic acid biosynthesis and metabolism in the sea urchin *Strongylocentrotus intermedius*. Sci Rep. 2020;10:1697. https://doi.org/10.1038/s41598-020-58643-x.
9. Zhadan PM, Vaschenko MA, Almyashova TN. Effects of environmental factors on reproduction of the sea urchin Strongylocentrotus intermedius. Sea urchin–from environment to aquaculture and biomedicine. Reijeka: INTECH. 2017;3:35–69.
10. Jiang X, Liu L, Guo H, Liu P, Tian W, Ou F, Ding J, Zhang W, Chang Y. Establishment of Parentage Identification Method for Sea Urchin *Strongylocentrotus intermedius* Based on SSR-seq Technology. Genes. 2024;15:630. https://doi.org/10.3390/genes15050630.
11. Kelly MS, Hunter AJ, Scholfield CL, McKenzie JD. Morphology and survivorship of larval Psammechinus miliaris (Gmelin) (Echinodermata: Echinoidea) in response to varying food quantity and quality. Aquaculture. 2000. https://doi.org/10.1016/s0044-8486(99)00296-3.
12. Li X, Qin Y, Xu Y. Color atlas of histology and embryology for aquatic animals. China Agricultural Press Ltd.); 2021;104-10. https://www.pwsannong.com/booklib/bookIntroduce?SiteID=123&ID=20369070.
13. Adema CM. Sticky problems: extraction of nucleic acids from molluscs. PHILOS T R SOC B. 2021;376:20200162. https://doi.org/10.1098/rstb.2020.0162.
14. Koren S, Walenz BP, Berlin K, Miller JR, Bergman NH, Phillippy AM. Canu: scalable and accurate long-read assembly via adaptive k-mer weighting and repeat separation. Genome Res. 2017;27:722–36. https://doi.org/10.1101/gr.215087.116.

15. Kurtz S, Phillippy A, Delcher AL, Smoot M, Shumway M, Antonescu C, Salzberg SL. Versatile and open software for comparing large genomes. Genome Biol. 2004;5:1–9. https://doi.org/10.1186/gb-2004-5-2-r12.
16. Li H, Durbin R. Fast and accurate short read alignment with Burrows-Wheeler transform. Bioinformatics. 2009;25:1754–60. https://doi.org/10.1093/bioinformatics/btp324.
17. Belton J-M, McCord RP, Gibcus JH, Naumova N, Zhan Y, Dekker J. Hi–C: a comprehensive technique to capture the conformation of genomes. Methods. 2012;58:268–76.
18. Burton JN, Adey A, Patwardhan RP, Qiu R, Kitzman JO, Shendure J. Chromosome-scale scaffolding of de novo genome assemblies based on chromatin interactions. Nat Biotechnol. 2013;31:1119–25. https://doi.org/10.1038/nbt.2727.
19. Simão FA, Waterhouse RM, Ioannidis P, Kriventseva EV, Zdobnov EM. BUSCO: assessing genome assembly and annotation completeness with single-copy orthologs. Bioinformatics. 2015;31. https://doi.org/10.1093/bioinformatics/btv351.
20. Price AL, Jones NC, Pevzner PA. De novo identification of repeat families in large genomes. Bioinformatics. 2005;1:351–8. https://doi.org/10.1093/bioinformatics/bti1018.
21. Bao W, Kojima KK, Kohany O. Repbase Update, a database of repetitive elements in eukaryotic genomes. Mob DNA. 2015;6:11. https://doi.org/10.1186/s13100-015-0041-9.
22. Tarailo-Graovac M, Chen N. Using RepeatMasker to identify repetitive elements in genomic sequences. Curr Protoc. 2009;4. https://doi.org/10.1002/0471250953.bi0410s25.
23. Dakouane-Giudicelli M, Legrand B, Bergere M, Giudicelli Y, Cussenot O, Selva J. Association between androgen receptor gene CAG trinucleotide repeat length and testicular histology in older men. FERTIL STERIL. 2006;86:873–7. https://doi.org/10.1016/j.fertnstert.2006.03.035.
24. Stanke M, Diekhans M, Baertsch R, Haussler D. Using native and syntenically mapped cDNA alignments to improve de novo gene finding. Bioinformatics. 2008;24:637–44. https://doi.org/10.1093/bioinformatics/btn013.
25. Korf I. Gene finding in novel genomes. BMC Bioinf. 2004;5:59. https://doi.org/10.1186/1471-2105-5-59.
26. Keilwagen J, Wenk M, Erickson JL, Schattat MH, Grau J, Hartung F. Using intron position conservation for homology-based gene prediction. Nucleic Acids Res. 2016;44:e89–89. https://doi.org/10.1093/nar/gkw092.
27. Tang S, Lomsadze A, Borodovsky M. Identification of protein coding regions in RNA transcripts. Nucleic Acids Res. 2015;43:e78–78. https://doi.org/10.1093/nar/gkv227.
28. Haas J, Delcher B, Mount LA, Wortman MS, Smith RJ Jr, R.K., et al. Improving the Arabidopsis genome annotation using maximal transcript alignment assemblies. Nucleic Acids Res. 2003;31:5654–66.
29. Haas BJ, Salzberg SL, Zhu W, Pertea M, Allen JE, Orvis J, White O, Buell CR, Wortman JR. Automated eukaryotic gene structure annotation using EVidenceModeler and the Program to Assemble Spliced Alignments. Genome Biol. 2008;9:R7. https://doi.org/10.1186/gb-2008-9-1-r7.
30. Lowe TM, Eddy SR. tRNAscan-SE: a program for improved detection of transfer RNA genes in genomic sequence. Nucleic Acids Res. 1997;25:955–64. https://doi.org/10.1093/nar/25.5.955.
31. She R, Chu JSC, Wang K, Pei J, Chen N. GenBlastA: enabling BLAST to identify homologous gene sequences. Genome Res. 2008;19:143–9. https://doi.org/10.1101/gr.082081.108.
32. Birney E, Clamp M, Durbin R. GeneWise and Genomewise. GENOME RES. 2004;14:988–95. https://doi.org/10.1101/gr.1865504.
33. Emms DM, Kelly S. OrthoFinder: phylogenetic orthology inference for comparative genomics. Genome Biol. 2019;20:238. https://doi.org/10.1186/s13059-019-1832-y.
34. Katoh K, Standley DM. A simple method to control over-alignment in the MAFFT multiple sequence alignment program. Bioinformatics. 2016;32:1993–1942. https://doi.org/10.1093/bioinformatics/btw108.
35. Suyama M, Torrents D, Bork P. PAL2NAL: robust conversion of protein sequence alignments into the corresponding codon alignments. Nucleic Acids Res. 2006;34:W609–12. https://doi.org/10.1093/nar/gkl315.
36. Van der Straeten J, De Brouwer W, Kabongo E, Dresse M-F, Fostier K, Schots R, Van Riet I, Bakkus M. Validation of a PCR-Based Next-Generation Sequencing Approach for the Detection and Quantification of Minimal Residual Disease in Acute Lymphoblastic Leukemia and Multiple Myeloma Using gBlocks as Calibrators. J MOL DIAGN. 2021;23:599–611. https://doi.org/10.1016/j.jmoldx.2021.01.009.
37. Minh BQ, Schmidt HA, Chernomor O, Schrempf D, Woodhams MD, von Haeseler A, Lanfear R. IQ-TREE 2: New Models and Efficient Methods for Phylogenetic Inference in the Genomic Era. Mol Biol Evol. 2020;37:1530–4. https://doi.org/10.1093/molbev/msaa015.
38. Puttick MN. MCMCtreeR: functions to prepare MCMCtree analyses and visualize posterior ages on trees. Bioinformatics. 2019;35:5321–2. https://doi.org/10.1093/bioinformatics/btz554.
39. Ye Q, Gao C, Xiao H, Ruan S, Wang Y, Li X, Chang Y, Zhao C, Wang H, Han B, Ding J. Feeding Behavior, Gut Microbiota, and Transcriptome Analysis Reveal Individual Growth Differences in the Sea Urchin Strongylocentrotus intermedius. Biology. 2024;13:705. https://doi.org/10.3390/biology13090705.
40. Kim D, Pertea G, Trapnell C, Pimentel H, Kelley R, Salzberg SL. TopHat2: accurate alignment of transcriptomes in the presence of insertions, deletions and gene fusions. Genome Biol. 2013;14:R36. https://doi.org/10.1186/gb-2013-14-4-r36.
41. Love MI, Huber W, Anders S. Moderated estimation of fold change and dispersion for RNA-seq data with DESeq2. Genome Biol. 2014;15:550. https://doi.org/10.1186/s13059-014-0550-8.
42. Sodergren E, Weinstock GM, Davidson EH, Cameron RA, Gibbs RA, Angerer RC, Angerer LM, Arnone MI, Burgess DR, Burke RD, et al. The genome of the sea urchin Strongylocentrotus purpuratus. Science. 2006;314:941–52. https://doi.org/10.1126/science.1133609.
43. Magri MS, Voronov D, Foley S, Martínez-García PM, Franke M, Cary GA, Santos-Pereira JM, Cuomo C, Fernández-Moreno M, Gil-Galvez A et a. Deep conservation of cis-regulatory elements and chromatin organization in echinoderms uncover ancestral regulatory features of animal genomes. bioRxiv - Evolutionary Biology, 2024 – 2011. https://doi.org/10.1101/2024.11.30.626178.
44. Kinjo S, Kiyomoto M, Yamamoto T, Ikeo K, Yaguchi S. HpBase: A genome database of a sea urchin, Hemicentrotus pulcherrimus. Dev Growth Differ. 2018;60:174–82. https://doi.org/10.1111/dgd.12429.
45. Davidson PL, Guo H, Wang L, Berrio A, Zhang H, Chang Y, Soborowski AL, McClay DR, Fan G, Wray GA. Chromosomal-Level Genome Assembly of the Sea Urchin Lytechinus variegatus Substantially Improves Functional Genomic Analyses. Genome Biol. Evol. 2020;12;1080–1086. https://doi.org/10.1093/gbe/ evaa101%J Genome Biology and Evolution.
46. Costantini M, Esposito R, Ruocco N, Caramiello D, Cordella A, Ventola GM, Zupo V. De novo assembly of the genome of the sea urchin *Paracentrotus lividus* (Lamarck 1816). 2024;25(3):1685. https://doi.org/10.3390/ijms25031685.
47. Polinski JM, Castellano KR, Buckley KM, Bodnar AG. Genomic signatures of exceptional longevity and negligible aging in the long-lived red sea urchin. Cell Rep. 2024;43:114021. https://doi.org/10.1016/j.celrep.2024.114021.
48. Zhang J, Guo Y, Su J, Yu G, Ma Z, Qin C. The first high-quality genome assembly and annotation of Anthocidaris crassispina. Sci Data. 2024;11:866. https://doi.org/10.1038/s41597-024-03733-y.
49. Chen X, Zhang W, Li Y, Liu L, Zhang B, Ding J, and Y., C. Methods for egg membrane and fertilization membrane removal and karyotype analysis of the sea urchin (*Strongylocentrotus intermedius*). J Fish Sci China. 2020;27:1033–41. (in Chinese).
50. UeharaT, Shingaki M, Taira K, Arakaki Y, Nakatomi H. Chromosome studies in eleven Okinawan species of sea urchins, with special reference to four species of the Indo-Pacific Echinometra. In: Yanagisawa T, editor.Biology of echinodermata. CRC Press; 2020. pp. 119–29. https://doi.org/10.1201/9781003077565-27.
51. Davidson PL, Lessios HA, Wray GA, McMillan WO, Prada C. Near-Chromosomal-Level Genome Assembly of the Sea Urchin Echinometra lucunter, a Model for Speciation in the Sea. GENOME BIOL EVOL. 2023;15:evad093. https://doi.org/10.1093/gbe/evad093.
52. Davidson PL, Guo H, Wang L, Berrio A, Zhang H, Chang Y, Soborowski AL, McClay DR, Fan G, Wray GA. Chromosomal-Level Genome Assembly of the Sea Urchin Lytechinus variegatus Substantially Improves Functional Genomic Analyses. GENOME BIOL EVOL. 2020;12:1080–6. https://doi.org/10.1093/gbe/evaa101.
53. Wang H, Zhao W, Ding B, Zhang Y, Huang X, Liu X, Zuo R, Chang Y, Ding J. Comparative lipidomics profiling of the sea urchin, Strongylocentrotus intermedius. Comp Biochem Physiol D: Genomics Proteom. 2021;40:100900. . https://doi.org/10.1016/j.cbd.2021.100900
54. Ding J, Yang D, Wang H, Zuo R, Qi S, Han L, Chang Y. Cloning, characterization and transcription analysis of fatty acyl desaturase (*Δ6Fad-like*) and elongase (*Elovl4-like, Elove5-like*) during embryos development of *Strongylocentrotus*

intermedius. Aquacult Res. 2019;50:3483–92. https://doi.org/10.1111/are.14316.
55. Han L, Ding J, Wang H, Zuo R, Quan Z, Fan Z, Liu Q, Chang Y. Molecular characterization and expression of SiFad1 in the sea urchin (Strongylocentrotus intermedius). Gene. 2019;705:133–41. https://doi.org/10.1016/j.gene.2019.04.043.
56. Morcillo S, Martín-Núñez GM, Rojo-Martínez G, Almaraz MC, García-Escobar E, Mansego ML, De Marco G, Chaves FJ, Soriguer F. *ELOVL6* genetic variation is related to insulin sensitivity: a new candidate gene in energy metabolism. PLoS ONE. 2011;6:e21198.
57. Monroig Ó, Tocher DR, Navarro JC. Biosynthesis of polyunsaturated fatty acids in marine invertebrates: recent advances in molecular mechanisms. Mar Drugs. 2013;11:3998–4018.
58. Kabeya N, Sanz-Jorquera A, Carboni S, Davie A, Oboh A, Monroig O. Biosynthesis of polyunsaturated fatty acids in sea urchins: molecular and functional characterisation of three fatty acyl desaturases from *Paracentrotus lividus* (Lamark 1816). PLoS ONE. 2017;12:e0169374.
59. Liu MY, Wang QC, Li JQ, Zhang D, Mu JH, Shen XH. Genome-Wide Identification and Comparative Analysis of Elongation of Very Long-Chain Fatty Acid (Elovl) Genes in Echinoderms. Russian J Genet. 2024;60:450–9.
60. Harayama T, Shimizu T. Roles of polyunsaturated fatty acids, from mediators to membranes. J Lipid Res. 2020;61:1150–60. https://doi.org/10.1194/jlr.R120000800.
61. Yotbuntueng P, Jiemsup S, Deenarn P, Tobwor P, Yongkiettrakul S, Vichai V, Pruksatrakul T, Sittikankaew K, Karoonuthaisiri N, Leelatanawit R, Wimuttisuk W. Differential distribution of eicosanoids and polyunsaturated fatty acids in the Penaeus monodon male reproductive tract and their effects on total sperm counts. PLoS ONE. 2022;17:e0275134. https://doi.org/10.1371/journal.pone.0275134.
62. Zuo R, Ning Y, Di W, Heqiu Y, Song J, Ding J, Chang Y. Effects of Dietary Lipid Sources on the Growth, Gonad Development, Fatty Acid Composition and Spawning Performance of Broodstock, and Early Larvae Quality of Sea Urchin (Strongylocentrotus intermedius). Front Mar Sci. 2022;9:927116. https://doi.org/10.3389/fmars.2022.927116.
63. Mukerjee S, Saeedan AS, Ansari MN, Singh M. Polyunsaturated Fatty Acids Mediated Regulation of Membrane Biochemistry and Tumor Cell Membrane Integrity. Membr (Basel). 2021;11:479. https://doi.org/10.3390/membranes11070479.
64. Wang H, Zhao W, Ding B, Zhang Y, Huang X, Liu X, Zuo R, Chang Y, Ding JJCB, Genomics PPD, and Proteomics. Comparative lipidomics profiling of the sea urchin. Strongylocentrotus intermedius. 2021;40:100900.
65. Calder PC. Eicosanoids Essays Biochem. 2020;64:423–41. https://doi.org/10.1042/ebc20190083.
66. Bhagavan NV. Medical biochemistry. AcademicPress; 2002. pp. 358-65. https://www.vitalsource.com/products/medical-biochemistry-bhagavan-n-v-v9780120954407.
67. Blanco A, Blanco G. Medical biochemistry. AcademicPress; 2017. pp. 292-30. https://www.sciencedirect.com/book/monograph/9780128035504/medical-biochemistry.
68. Nhan HT, Nhu TQ, Duc PM, Liew HJ, Ako H, Jha R. Effects of dietary arachidonic acid on final maturation, spawning and composition of gonad of black sea urchin Diadema setosum (Leske, 1778). Aquacult Nutr. 2020;26:1771–9. https://doi.org/10.1111/anu.13127.
69. Zuo R, Li M, Ding J, Chang Y. Higher dietary arachidonic acid levels improved the growth performance, gonad development, nutritional value, and antioxidant enzyme activities of adult sea urchin (Strongylocentrotus intermedius). J Ocean Univ China. 2018;17. https://doi.org/10.1007/s11802-018-3606-7.
70. Jiang Y, Hu Y, Xu W, Luo H, Chen J, Tao B, Luo D, Han D, Zhu X, Xie S. Effects of dietary arachidonic acid on growth, gonadal development, and tissue fatty acid composition in the hermaphroditic swamp eel (Monopterus albus). Aquacult Rep. 2023;33:101791.
71. Zuo R, Li M, Ding J, Chang Y. Higher Dietary Arachidonic Acid Levels Improved the Growth Performance, Gonad Development, Nutritional Value, and Antioxidant Enzyme Activities of Adult Sea Urchin (*Strongylocentrotus intermedius*). J Ocean Univ China. 2018;17:932–40. https://doi.org/10.1007/s11802-018-3606-7.
72. Wang Z, Wang G, Ge H, Zhang L. Effects of various natural diets on gonad development, roe quality, and intestinal microbiota of the purple sea urchin (Heliocidaris crassispina). Aquacult Nutr. 2025(3196037). https://doi.org/10.1155/anu/3196037.
73. Oliveira EF, Araújo BC, Marques VH, de Mello PH, Moreira RG, Honji RM. Influence of Docosahexaenoic and Eicosapentaenoic Acid Ratio and Temperature on the Growth Performance, Fatty Acid Profile, and Liver Morphology of Dusky Grouper (Epinephelus marginatus) (Teleostei: Serranidae) Juveniles. Anim (Basel). 2023;13:3212. https://doi.org/10.3390/ani13203212.
74. Levitan DR. The distribution of male and female reproductive success in a broadcast spawning marine invertebrate. Integr Comp Biol. 2005;45:848–55.
75. Zhadan PM, Vaschenko MA, Ryazanov SD. Assessing the effect of environmental factors on the spawning activity of the sea urchin Strongylocentrotus intermedius through video recording observations. Mar Ecol Prog Ser. 2018;588:101–19.
76. Levitan DR. Sperm velocity and longevity trade off each other and influence fertilization in the sea urchin Lytechinus variegatus. Proc R Soc Lond B Biol Sci. 2000;267:531–4.
77. Kozhina V, Terekhova T, Svetashev V. Lipid composition of gametes and embryos of the sea urchin Strongylocentrotus intermedius at early stages of development. Dev Biol. 1978;62:512–7.
78. Rahman MA, Yusoff FM, Arshad A, Shamsudin MN, Amin S. Embryonic, larval, and early juvenile development of the tropical sea urchin, Salmacis sphaeroides (Echinodermata: Echinoidea). The Scientific World Journal. 2012;1:938482. https://doi.org/10.1100/2012/938482.
79. Marshall DJ, Keough MJ. The evolutionary ecology of offspring size in marine invertebrates. Adv Mar Biol. 2007;53:1–60.
80. Tu Q, Cameron RA, Davidson EH. Quantitative developmental transcriptomes of the sea urchin *Strongylocentrotus purpuratus*. Dev Biol. 2013;385:160–7. https://doi.org/10.1016/j.ydbio.2013.11.019.
81. Hogan JD, Keenan JL, Luo L, Ibn-Salem J, Lamba A, Schatzberg D, Piacentino ML, Zuch DT, Core AB, Blumberg C, et al. The developmental transcriptome for Lytechinus variegatus exhibits temporally punctuated gene expression changes. Dev Biol. 2019;460:139–54. https://doi.org/10.1016/j.ydbio.2019.12.002.
82. Jackson D, Leys SP, Hinman VF, Woods R, Lavin MF, Degnan BM. Ecological regulation of development: induction of marine invertebrate metamorphosis. Int J Dev Biol. 2002;46:679–86.
83. Cocurullo M, Paganos P, Wood NJ, Arnone MI, Oliveri P. Molecular and cellular characterization of the TH pathway in the Sea urchin Strongylocentrotus purpuratus. Cells. 2023;12:272.
84. Chen M, Huang G, QI H, Liu X, Xu Y. Research progress of benthic diatoms on sandy beach. Ecol Sci. 2024;43:246. https://doi.org/10.14108/j.cnki.1008-8873.2024.02.027.
85. Doll PC, Caballes CF, Hoey AS, Uthicke S, Ling SD, Pratchett MS. Larval settlement in echinoderms: a review of processes and patterns. Oceanography and Marine Biology; 2022. pp. 433– 94. https://doi.org/10.1201/9781003288602-9.
86. Monroig Ó, Shu-Chien A, Kabeya N, Tocher DR, Castro LFC. Desaturases and elongases involved in long-chain polyunsaturated fatty acid biosynthesis in aquatic animals: From genes to functions. Prog Lipid Res. 2022;86:101157.
87. Yaguchi S, Kanoh K, Amemiya S, Katow H. Initial analysis of immunochemical cell surface properties, location and formation of the serotonergic apical ganglion in sea urchin embryos. Dev Growth Differ. 2000. https://doi.org/10.1046/j.1440-169x.2000.00535.x.
88. Heyland A, Schuh N, Rast J. Sea Urchin Larvae as a Model for Postembryonic Development. Result Probl Cell Differ. 2018. https://doi.org/10.1007/978-3-319-92486-1_8.
89. Miao R, Li M, Zhang Q, Yang C, Wang X. An ECM-to-Nucleus Signaling Pathway Activates Lysosomes for C. elegans Larval Development. Dev Cell. 2019. https://doi.org/10.1016/j.devcel.2019.10.020.

Publisher's note